

## ORIGINAL ARTICLE

# Transactivation of *bad* by vorinostat-induced acetylated p53 enhances doxorubicin-induced cytotoxicity in cervical cancer cells

Sook-Jeong Lee<sup>1,5</sup>, Sung-Ook Hwang<sup>2,5</sup>, Eun Joo Noh<sup>1,5,6</sup>, Dong-Uk Kim<sup>3</sup>, Miyoung Nam<sup>1</sup>, Jong Hyeok Kim<sup>4</sup>, Joo Hyun Nam<sup>4</sup> and Kwang-Lae Hoe<sup>1</sup>

Vorinostat (VOR) has been reported to enhance the cytotoxic effects of doxorubicin (DOX) with fewer side effects because of the lower DOX dosage in breast cancer cells. In this study, we investigated the novel mechanism underlying the synergistic cytotoxic effects of VOR and DOX co-treatment in cervical cancer cells HeLa, CaSki and SiHa cells. Co-treatment with VOR and DOX at marginal doses led to the induction of apoptosis through caspase-3 activation, poly (ADP-ribose) polymerase cleavage and DNA micronuclei. Notably, the synergistic growth inhibition induced by the co-treatment was attributed to the upregulation of the pro-apoptotic protein Bad, as the silencing of Bad expression using small interfering RNA (siRNA) abolished the phenomenon. As siRNA against p53 did not result in an increase in acetylated p53 and the consequent upregulation of Bad, the observed Bad upregulation was mediated by acetylated p53. Moreover, a chromatin immunoprecipitation analysis showed that the co-treatment of HeLa cells with VOR and DOX increased the recruitment of acetylated p53 to the *bad* promoter, with consequent *bad* transactivation. Conversely, C33A cervical cancer cells containing mutant p53 co-treated with VOR and DOX did not exhibit Bad upregulation, acetylated p53 induction or consequent synergistic growth inhibition. Together, the synergistic growth inhibition of cervical cancer cell lines induced by co-treatment with VOR and DOX can be attributed to the upregulation of Bad, which is induced by acetylated p53. These results show for the first time that the acetylation of p53, rather than histones, is a mechanism for the synergistic growth inhibition induced by VOR and DOX co-treatments.

*Experimental & Molecular Medicine* (2014) 46, e76; doi:10.1038/emm.2013.149; published online 14 February 2014

**Keywords:** bad; cervical cancer cell; doxorubicin; p53 acetylation; vorinostat

## INTRODUCTION

The anthracycline doxorubicin (DOX) is known to be an effective chemotherapy drug for a wide variety of cancers by inducing topoisomerase II-mediated DNA breaks.<sup>1</sup> Despite extensive clinical use, its application is hampered by dose-dependent side effects.<sup>2</sup> Indeed, DOX often complicates cancer treatment because therapeutic dosages must be limited in order to maintain patients' quality of life. Thus, novel therapeutic strategies to obtain maximum efficacy at a lower DOX dosage have been proposed, including the combined treatment of cervical cancer with interferon- $\alpha$ .<sup>3</sup> Histone deacetylase inhibitors (HDIs) are a new class of promising

anticancer agents that induce acetylation of the histones and non-histone proteins that are involved in the regulation of gene expression and various cellular pathways.<sup>4</sup> In particular, vorinostat (VOR, also known as suberoylanilide hydroxamic acid) has been approved for hematological malignancies by the United States Food and Drug Administration.<sup>5</sup>

Cervical cancer is one of the most common gynecological cancers and a leading cause of death among women.<sup>6</sup> Human papilloma virus (HPV) DNA is detected in over 90% of all cervical cancers, suggesting that cervical carcinogenesis is caused by HPV infection.<sup>7</sup> The role of HPV in carcinogenesis is via the functional inactivation of the p53 tumor

<sup>1</sup>Department of New Drug Discovery and Development, Chungnam National University, Daejeon, Republic of Korea; <sup>2</sup>Department of Obstetrics and Gynecology, Inha University Hospital, Incheon, Republic of Korea; <sup>3</sup>Aging Research Center, Korea Research Institute of Bioscience and Biotechnology (KRIBB), Daejeon, Republic of Korea and <sup>4</sup>Department of Obstetrics and Gynecology, Asan Medical Center, Seoul, Republic of Korea

<sup>5</sup>These authors contributed equally to this work.

<sup>6</sup>Current address: Biotechnology examination division, Korean Intellectual Property Office (KIPO), Daejeon, 302-701, Republic of Korea.

Correspondence: Professor K-L Hoe, Department of New Drug Discovery and Development, Chungnam National University, 99 Daehak-ro, Yuseong, Daejeon 305-764, Republic of Korea.

E-mail: kwanghoe@cnu.ac.kr

Received 24 June 2013; revised 24 October 2013; accepted 25 October 2013

suppressor, which orchestrates such cellular responses as cell cycle arrest, DNA repair and apoptosis upon genotoxic damage by chemotherapy drugs.<sup>8</sup> The p53 protein, a short-lived protein, is stabilized and activated via post-translational modifications, including phosphorylation, acetylation and sumoylation.<sup>9</sup> In particular, the acetylation of p53 promotes the transcriptional activation of target genes by enhancing the DNA-binding ability of p53 and the recruitment of co-activators.<sup>10</sup> Many p53-inducible genes have been identified over the past two decades, some of which are members of the Bcl-2 family, including the pro-apoptotic Bad protein.<sup>11</sup> In response to DNA damage, p53 binds directly to the *bad* promoter region residing ~6.6 kb upstream of the start codon to upregulate *bad* transcription.<sup>11,12</sup>

Previous reports have shown that the pretreatment of breast cancer cells with HDIs enhances the cytotoxic effects of small molecules, such as cisplatin and DOX.<sup>13,14</sup> A plausible explanation for such sequence-specific potentiation is that histone acetylation by HDIs relaxes the chromatin structure, allowing the access of DNA-targeting anticancer drugs to the cancer cell DNA. However, the detailed mechanisms of combined DOX and VOR treatment are not completely understood. In the present study, we investigated a novel mechanism underlying the synergistic growth inhibition effects by the co-treatment of human cervical cancer cell lines with VOR and DOX.

## MATERIALS AND METHODS

### Cell culture and chemicals

The human cervical cancer line HeLa was obtained from the American Type Culture Collection (Manassas, VA, USA). The other cell lines, SiHa, CaSki and C33A, were obtained from the Korean Cell Line Bank (Seoul, Korea). The cells were grown in Dulbecco's Modified Eagle Medium supplemented with 10% fetal bovine serum and 1% penicillin/streptomycin at 37 °C in a humidified atmosphere containing 5% CO<sub>2</sub>.

The reagents for cell culture and general chemicals were purchased from Life Technologies (Gibco, Grand Island, NY, USA) and Sigma-Aldrich (St Louis, MO, USA), respectively, unless otherwise stated. DOX and VOR were generously provided by Dr Choi YW at the Korea United Pharmacy (Seoul, Korea).

### MTT (3-(4,5-dimethylthiazol-2-yl)-2,5-diphenyltetrazolium bromide) assay

Cervical cancer cells (~10<sup>4</sup> cells per well in a 96-well plate) were treated with VOR and/or DOX at the indicated concentrations, and their viability was measured using the MTT assay. Briefly, 10 µl of MTT stock solution (5 mg ml<sup>-1</sup> in phosphate-buffered saline) was added to each well, followed by incubation at 37 °C for 3 h to allow the cell-mediated reduction of MTT. To detect the amount of reduced MTT, 100 µl of dimethyl sulfoxide was added, and the absorbance was measured at 540 nm using a micro-plate reader.

### Isobologram analysis

To determine the synergistic cytotoxic effect of co-treatment with VOR and DOX, we performed an isobologram analysis, as described previously.<sup>15</sup> Briefly, the ED<sub>30</sub> value of each compound was determined, and each ED<sub>30</sub> was then plotted on each axis of the

graph. A diagonal line was drawn between the two ED<sub>30</sub> spots of each single treatment of VOR and DOX, representing the line of additivity as a control. Several data sets corresponding to the same ED<sub>30</sub> after treatments with various concentrations of VOR and DOX in combination were plotted as dots on the graph. The results indicate synergy, additivity or antagonism when the dots are located below, on or above the diagonal line, respectively.

### 5 Fluorescence-activated cell sorting (FACS) analysis

Cell viability was measured using the FACS Calibur (BD Biosciences Immunocytometry Systems; San Jose, CA, USA), following a modified protocol (Sigma-Aldrich). Briefly, cervical cancer cells were treated with VOR and/or DOX for 24 h at 37 °C in a humidified CO<sub>2</sub> incubator. After the incubation, the cells were harvested using centrifugation and washed twice with cold phosphate-buffered saline. The cells were then incubated with Annexin V-FITC in a binding buffer (10 mM HEPES/NaOH, pH 7.5, containing 140 mM NaCl and 2.5 mM CaCl<sub>2</sub>) for 10 min at room temperature in the dark. The cells were sorted using the FACS Calibur Flow Cytometer to determine the live and apoptotic cell populations. The results were analyzed using CellQuest Pro software (BD Biosciences).

### Immunoblotting

Cells were treated and then lysed in a buffer containing 50 mM Tris (pH 8.0), 150 mM NaCl and 1% NP-40 plus a protease inhibitor cocktail tablet (Roche, Penzberg, Germany). The proteins were resolved using sodium dodecyl sulfate-polyacrylamide gel electrophoresis and transferred to nitrocellulose membranes. After a blocking treatment, the membranes were incubated with primary antibodies (1:1000 dilution) and then with horseradish peroxidase-conjugated secondary antibodies. Antibodies against cleaved caspase-3 and p53 acetylated at Lys382 (Ac-p53) were purchased from Cell Signaling Technology (Danvers, MA, USA). An antibody against poly (ADP-ribose) polymerase was purchased from BD Biosciences. Antibodies against Bcl-2, Bad, p53 and β-actin were purchased from Santa Cruz Biotechnology (Dallas, TX, USA), and an antibody against acetylated histone-3 was purchased from Merck Millipore (Billerica, MA, USA). The blots were developed using an enhanced chemiluminescence kit (GE Healthcare Life Science, Fairfield, CT, USA).

### Small interfering RNA assay

The oligonucleotide sequences of designed small interfering RNAs (siRNAs) are as follows: *bad* sense, 5'-GCGAGCCAGGUUUAAACC GU(dTdT)-3', and antisense, 5'-ACGGUUAACCUGGCUCG-C (dTdT)-3'; p53 sense, 5'-CACUACAACUACAUGUGUA(dTdT)-3', and antisense, 5'-UAC-ACAUGUAGUUAUAGUG(dTdT)-3'; negative control sense, 5'-GGCCUCAGCUGCGCG-ACGC(dTdT)-3', and antisense, 5'-GCGUCGCGCAGCUGAGGCC(dTdT)-3'. The siRNAs were synthesized and sequenced by Bioneer (Seoul, Korea). siRNA transfection was performed using the HiPerfect kit (Qiagen, Hilden, Germany) according to the manufacturer's instructions. After incubation for 48 h, the transfected cells were treated with 2.5 µM VOR and/or 0.2 µM DOX.

### Chromatin immunoprecipitation (ChIP) assay

The ChIP assay was performed using an immunoprecipitation kit (Merck Millipore) according to the manufacturer's instructions. Briefly, protein-bound chromatin DNA was prepared by the sonication of 1% formaldehyde-fixed cells. After pre-clearing, the DNA fragments were immunoprecipitated using antibodies against p53 and

acetylated p53 (Ac-p53). Immunoprecipitations without antibody (no Ab) and with IgG (IgG) were performed as negative controls; 0.5% of the total chromatin sample before immunoprecipitation (input) and the polymerase chain reaction (PCR) product of the pull-down complex using an antibody against acetylated histone-3 were employed as positive controls. DNA samples were prepared from the pull-down complexes by adding elution buffer, and the purified DNA samples were used as the templates for PCR. After an initial denaturation at 95 °C for 5 min, 30 cycles of denaturation at 95 °C for 30 s, annealing at 55 °C for 30 s, and extension at 72 °C for 45 s were performed. The PCR primer sequences used for the *bad* promoter are sense, 5'-GGAACCCGGTGGGGCCA-3', and antisense, 5'-ACCAGTAGCG-GGTGGTC-3'.

### RNA isolation and reverse transcriptase-PCR

After HeLa cells were treated with VOR and/or DOX for 16 h, total RNA was isolated using the RNeasy mini kit (Qiagen) according to the manufacturer's instructions. Complementary DNA was synthesized using 2 µg of total RNA, and the transcription levels were analyzed using PCR. The primer sequences are as follows: glyceraldehyde-3-phosphate dehydrogenase (*gapdh*, used as a normalization control) sense, 5'-GTCAACGGATTGGTCTGTATT-3', and antisense, 5'-AGTCTTCTGGGTGGCAGTGAT-3'; *bad* sense, 5'-ATGTTCCAGATCCCAGAGTTTG-3', and antisense, 5'-GTTCCGATCCCA CCAGGACT-3'. PCR was performed by annealing at 57 °C for 27 cycles for *bad* and 24 cycles for *gapdh*, respectively.

### Statistical analysis

All the experiments were performed with triplicate samples and repeated at least three times. The data are presented as the mean ± s.d., and statistical comparisons between the groups were performed using Student's *t*-test. A *P*-value <0.05 was considered significant.

## RESULTS

### Co-treatment with VOR and DOX exerts synergistic growth inhibition on human cervical cancer cells

An isobologram analysis was performed to investigate the effects of VOR and DOX on synergistic growth inhibition. As a prerequisite, the optimal single dose of VOR or DOX resulting in ~70% HeLa cell viability after 24 h of treatment was determined. As shown in Supplementary Figure 1, the optimal co-treatment doses of VOR and DOX were determined to be 2.5 µM for VOR (upper box) and 0.2 µM for DOX (lower box). According to the results of the isobologram analysis, all the data points of the co-treatments were located below the diagonal line, indicating the synergistic effect of VOR and DOX in HPV16-infected cervical cancer HeLa cells, HPV18-infected cervical cancer cells (CaSki and SiHa) and human osteosarcoma U2OS cells (Figure 1a). Consistent with the observed synergistic growth inhibition, the co-treatment of HeLa cells with 2.5 µM VOR and 0.2 µM DOX resulted in the typical signs of apoptosis induction, including DNA fragmentation and deformed nuclei (Supplementary Figure 2). Furthermore, the synergistic effects of the co-treatments caused a prominent increase in the apoptotic cell population compared with the single treatments at marginal doses, as judged by Annexin V-FITC FACS analysis (Figure 1b).

### Synergistic growth inhibition can be attributed to apoptosis induction mediated by cleaved caspase-3 and poly (ADP-ribose) polymerase via upregulation of the pro-apoptotic protein Bad

The above results prompted us to examine which factors are related to the induction of apoptosis. As shown by the arrows in Figure 2a, co-treatment resulted in the induction of cleaved caspase-3 and poly (ADP-ribose) polymerase ( $P<0.001$ ), suggesting the involvement of the mitochondria-mediated pathway of apoptosis. However, each single treatment at the indicated doses did not activate the cleavage of caspase-3 (Figure 2a and upright arrows in Figure 2b). Next, we examined which Bcl-2 family members are regulated by the co-treatment. As expected, co-treatment resulted in a significant downregulation of the anti-apoptotic protein Bcl-2 ( $P<0.001$ ) and upregulation of the pro-apoptotic protein Bad ( $P<0.001$ , left panels in Figure 2c). Furthermore, the results of reverse transcriptase-PCR indicated that co-treatment led to a significant increase in the transcription level of *bad* compared with the *gapdh* normalization control ( $P<0.001$ , right panels in Figure 2c). Furthermore, Bad upregulation because of VOR and DOX co-treatment was confirmed by a siRNA analysis. Knockdown of Bad abolished the synergistic growth inhibition of HeLa cells ( $P<0.001$ , Figure 2d), SiHa, CaSki and U2OS cells and even DOX-resistant MCF7 cells (Supplementary Figure 3). Together, the data suggest that the synergistic growth inhibition induced by VOR and DOX co-treatment can be attributed to apoptosis induction mediated by the upregulation of the pro-apoptotic protein Bad.

### The increase in acetylated p53 mediates Bad upregulation

According to previous reports, p53 affects the regulation of Bcl-2 family molecules, and the acetylation of p53 results in *bad* transactivation.<sup>10-12</sup> These reports prompted us to investigate whether the Bad upregulation induced by the co-treatment of VOR and DOX is related to an increase in the acetylated form of p53 in HeLa (left panels in Figure 3a) and CaSki cells (right panels in Figure 3a). Expectedly, only co-treatment with VOR and DOX massively induced both Bad and acetylated p53 ( $P<0.001$ ). In contrast, a single VOR treatment slightly induced acetylated p53, without an increase in Bad ( $P<0.001$  and  $P<0.01$  in each cell), and a single DOX treatment induced both acetylated p53 and native p53, with a slight increase in Bad ( $P<0.05$ ). As a positive control, the single VOR treatment strongly induced the acetylation of histone-3 ( $P<0.001$  and  $P<0.01$  in each cell, respectively). These results suggest that the Bad upregulation induced by the co-treatment is related to increases in acetylated p53. To investigate the underlying mechanism of Bad upregulation, an siRNA analysis of *p53* was performed in HeLa cells. Compared with the control, knockdown of p53 abrogated the Bad upregulation stimulated by the co-treatment ( $P<0.001$ , Figure 3b). These results also suggest that the participation of p53 is crucial for the upregulation of Bad induced by VOR and DOX co-treatments via acetylated p53.

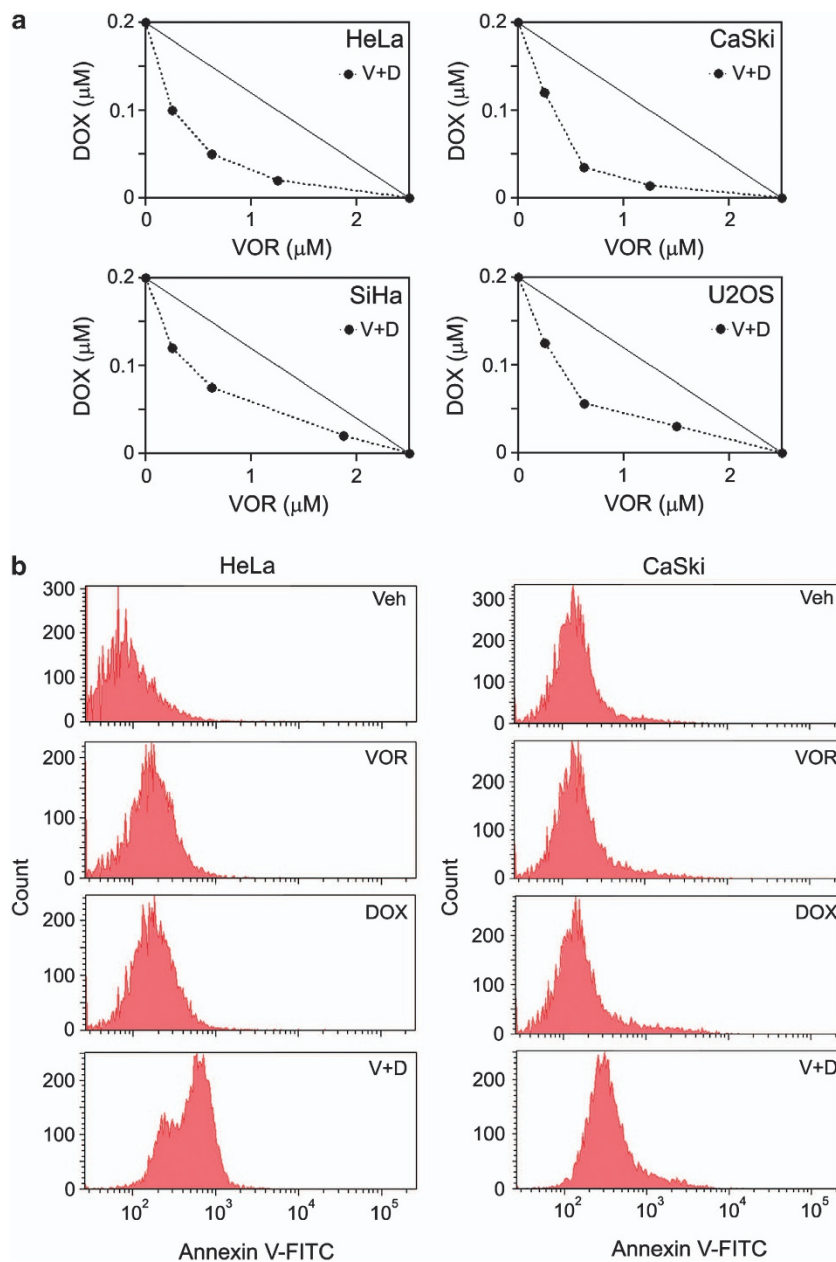


**Figure 1** VOR enhances DOX-induced cytotoxicity in several cancer cell lines. **(a)** Isobologram analysis was performed to assess the synergistic cytotoxic effects between VOR and DOX. Three cervical cancer cell lines, HeLa, CaSki and SiHa, as well as the osteosarcoma cell line U2OS, were co-treated for 24 h at various combinations of concentrations. Notably, all four cancer cell lines showed synergistic cytotoxic effects, as the data sets (●) are located below the control line (a straight line). The data points in the isobologram are the mean values of four independent replicates. V = VOR, D = DOX. **(b)** HeLa or CaSki cells were treated with vehicle, 2.5 μM VOR, and/or 0.2 μM DOX for 24 h, and FACS analysis was performed with 0.5 μg ml<sup>-1</sup> Annexin V-FITC to assess the apoptotic cell population. Compared with the single treatments, VOR and DOX co-treatments notably increased the Annexin V-FITC-positive cell populations. Veh = vehicle, V = VOR, D = DOX.

### Acetylated p53 enhances its recruitment and binding to the *bad* promoter

p53 was identified as the first non-histone protein that can be acetylated, and the status of p53 acetylation regulates its DNA-binding activity.<sup>10</sup> Thus, we examined whether acetylated p53, and not p53 itself, was critical for the upregulation of Bad using a ChIP assay of the *bad* promoter. As shown in Figure 4a, only acetylated p53 showed massive recruitment

and binding to the *bad* promoter ( $P < 0.001$ ), whereas p53 itself showed little recruitment and binding compared with the negative and positive controls ( $P < 0.05$ ). These results suggest that the recruitment of acetylated p53 to the *bad* promoter is crucial for the transactivation of *bad*.

It has been suggested that the cytotoxicity of chemotherapy drugs varies in cervical cancer cells depending on the p53 status.<sup>16,17</sup> In addition, our data (Figure 3c) showed that the



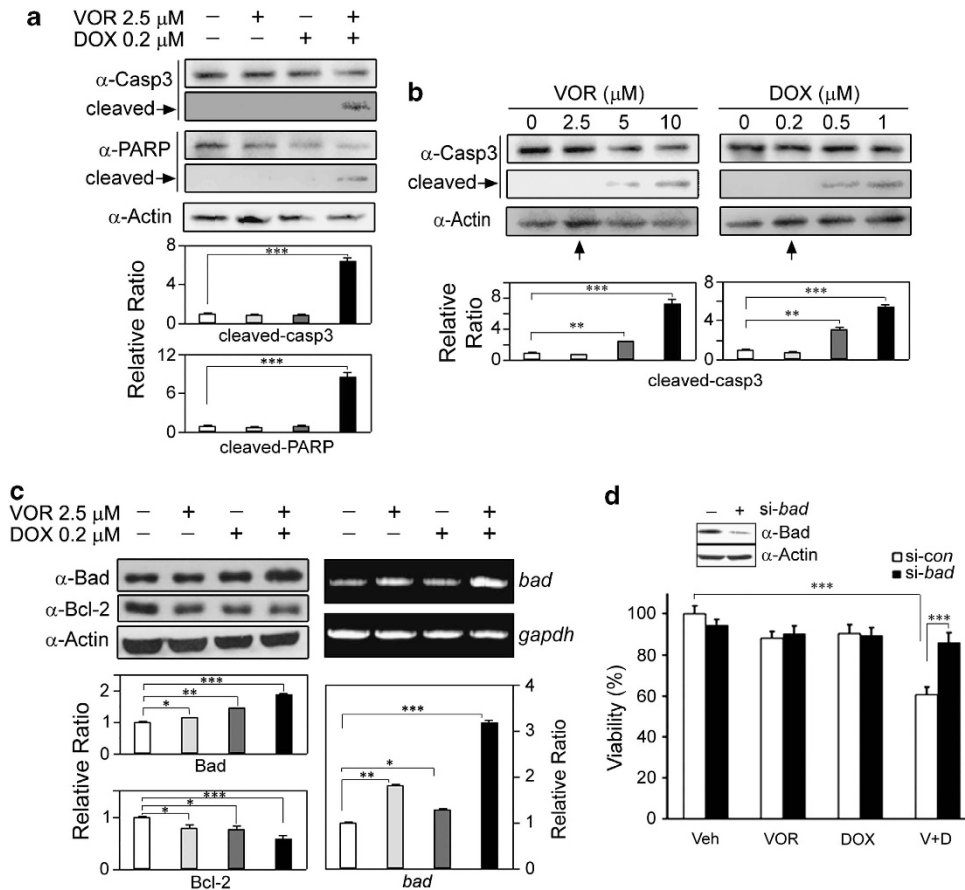


**Figure 2** Typical apoptotic markers, such as cleaved caspase-3 and poly (ADP-ribose) polymerase (PARP), are induced by the co-treatment, which is correlated with Bad upregulation. **(a)** HeLa cells were treated with 2.5  $\mu$ M VOR and/or 0.2  $\mu$ M DOX, and the activation of caspase-3 and PARP was assessed using a western blot analysis. Notably, each treatment alone did not induce activation of caspase-3 and PARP, whereas the co-treatment induced cleaved caspase-3 and PARP, typical apoptotic markers. The bars denote the changes in the density ratio of cleaved caspase-3 (cleaved-casp3) or cleaved PARP (cleaved-PARP) over  $\beta$ -actin ( $***P < 0.001$  versus vehicle;  $n = 5$ ). **(b)** HeLa cells were treated with VOR or DOX at the indicated concentrations for 16 h, and the concentrations that did not induce the cleavage of caspase-3 were determined using a western blot analysis. Notably, activation of caspase-3 was not observed until 2.5  $\mu$ M VOR and 0.2  $\mu$ M DOX were applied (upright arrows) ( $**P < 0.01$ ,  $***P < 0.001$  versus vehicle;  $n = 5$ ). **(c)** HeLa cells were treated with 2.5  $\mu$ M VOR and/or 0.2  $\mu$ M DOX for 16 h, and the upregulation of Bad and downregulation of Bcl-2 were observed using a western blot analysis (left panels). Additionally, the transcript level of *bad* was assessed with reverse transcriptase-PCR using *gapdh* as a normalization control (right panels) ( $*P < 0.05$ ,  $**P < 0.01$ ,  $***P < 0.001$  versus vehicle;  $n = 4$ ). **(d)** HeLa cells were transfected with *bad* (si-*bad*) or scrambled (si-con) siRNA for 48 h, followed by a 16-h treatment with 2.5  $\mu$ M VOR and/or 0.2  $\mu$ M DOX. The effects of the co-treatment on synergistic growth inhibition were observed with the MTT assay. The knockdown of Bad in the siRNA-transfected cells was evaluated using a western blot analysis (inset). Notably, transfection with an siRNA targeting *bad* abrogated the synergistic growth inhibition induced by the VOR and DOX co-treatments. The same result was observed in SiHa, CaSki and U2OS cells and even in DOX-resistant MCF7 breast cancer cells (Supplementary Figure 3) ( $***P < 0.001$  versus vehicle or si-con of V  $\pm$  D,  $n = 4$ ). Veh = vehicle, V = VOR, D = DOX.

participation of p53 is crucial for Bad upregulation. Thus, using C33A HPV-negative cervical cancer cells harboring mutations in *p53*, we confirmed that the participation of p53 is also critical for the synergistic growth inhibition induced by VOR and DOX co-treatments. Expectedly, when co-treated with VOR and DOX, the C33A cells showed no signs of apoptosis, such as the induction of cleaved poly (ADP-ribose) polymerase and activation of caspase-3 (data not shown). Similarly, the upregulation of Bad and induction of acetylated p53 were observed, despite the presence of p53 in the C33A cells (Figure 4b). Furthermore, the co-treatment of C33A cells

with VOR and DOX did not exert a synergistic growth inhibition and only showed an additive effect (Figure 4c). Additionally, the co-treatment did not result in cytotoxic effects on C33A cells (Figure 4d), whereas it was effective in HeLa, CaSki and SiHa cells (Figure 1b). These data confirm that the participation of native p53 is crucial for the synergistic growth inhibition of cancer cells induced by co-treatment with VOR and DOX. Together, the observed synergistic growth inhibition can be attributed to an increase in acetylated p53 and the consequent upregulation of Bad via the enhanced recruitment of acetylated p53 to the *bad* promoter.

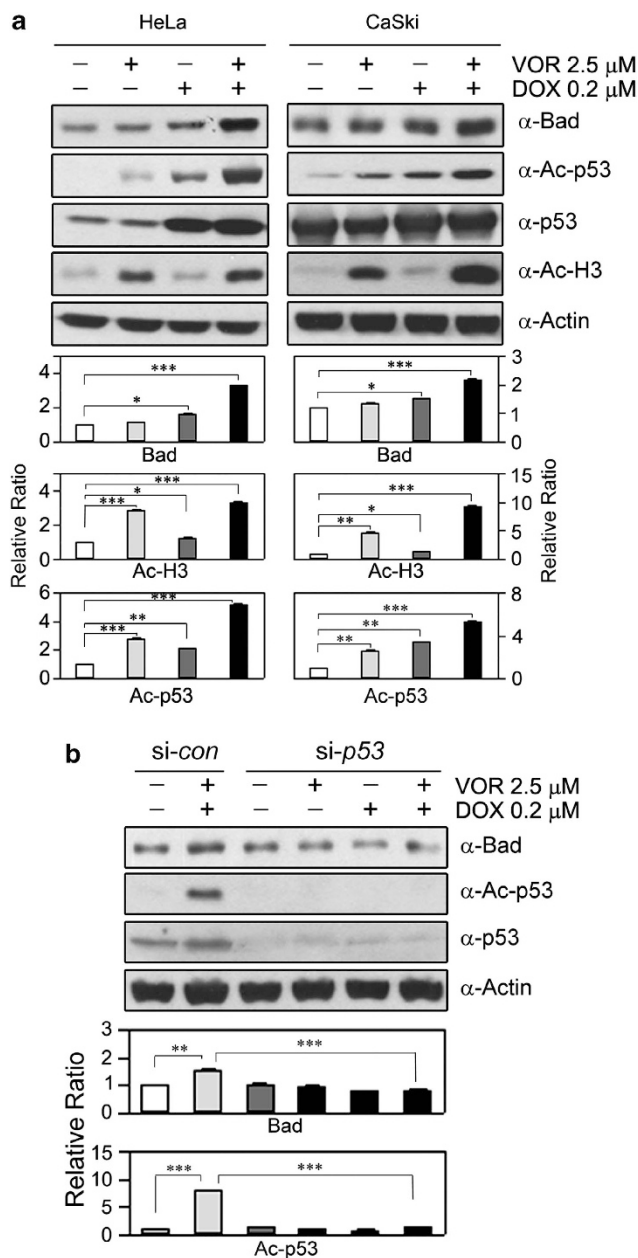


**Figure 3** The upregulation of Bad by co-treatment with VOR and DOX can be attributed to an increase in acetylated p53. (a) HeLa and CaSki cells were treated with 2.5  $\mu$ M VOR and/or 0.2  $\mu$ M DOX for 16 h, and the expression levels of acetylated p53 and Bad were analyzed. Notably, co-treatment with 2.5  $\mu$ M VOR and 0.2  $\mu$ M DOX induced the upregulation of both Bad and acetylated p53 ( $*P < 0.05$ ,  $**P < 0.01$ ,  $***P < 0.001$  versus vehicle;  $n = 4$ ). (b) HeLa cells were transfected with *p53* (si-*p53*) or scrambled (si-*con*) siRNA for 48 h, followed by a 16-h treatment with 2.5  $\mu$ M VOR and/or 0.2  $\mu$ M DOX. The expression level of Bad and acetylation level of p53 were then analyzed. The siRNA against *p53* caused knockdown of p53, leading to a reduction in acetylated p53 and consequently no upregulation of Bad, even for the co-treatment with VOR and DOX ( $**P < 0.01$ ,  $***P < 0.001$  versus vehicle or co-treated si-*con*;  $n = 4$ ).

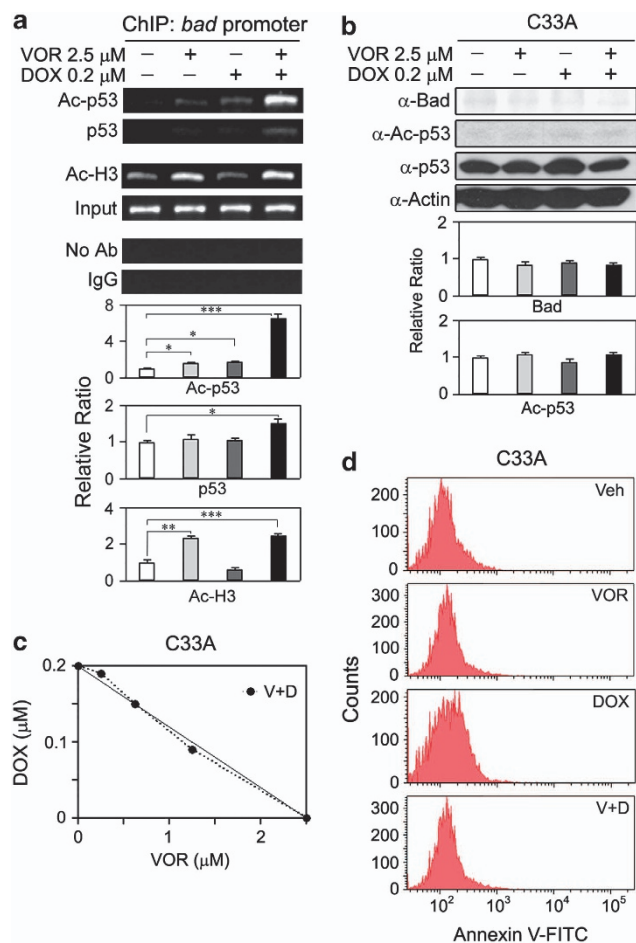


**Figure 4** Acetylated p53 has key roles in the transactivation of *bad* via enhanced recruitment to the *bad* promoter. (a) HeLa cells were treated with 2.5  $\mu$ M VOR and/or 0.2  $\mu$ M DOX for 8 h, and the binding activity of acetylated p53 to the *bad* promoter was analyzed using a ChIP assay. Only acetylated p53 exhibited strong recruitment and binding to the *bad* promoter ( $*P < 0.05$ ,  $**P < 0.01$ ,  $***P < 0.001$  versus vehicle;  $n = 3$ ). (b) C33A cells harboring mutations in the p53 protein were treated with 2.5  $\mu$ M VOR and/or 0.2  $\mu$ M DOX for 16 h, and the cell extracts were subjected to a western blot analysis to assess the expression levels of Bad, p53 and acetylated p53. Notably, the co-treatment of p53-mutated C33A cells with VOR and DOX did not result in an increase in the expression level of Bad or the acetylation level of p53, even in the presence of p53 ( $n = 4$ ). (c) C33A cells were co-treated with VOR and DOX for 24 h at various combinations of concentrations, and an isobologram analysis was performed to examine the synergistic effect of VOR and DOX co-treatments. The C33A cells defective in p53 only showed an additive effect and not a synergistic effect, as all the data sets ( $\bullet$ ) are located on the diagonal lines. The data points in the isobologram are the mean values of four independent replicates. (d) C33A cells were treated with vehicle, 2.5  $\mu$ M VOR, and/or 0.2  $\mu$ M DOX for 24 h. The cells were collected and incubated with 0.5  $\mu$ g ml $^{-1}$  of Annexin V-FITC, and FACS analysis was performed to detect apoptosis. The co-treatment of C33A with VOR and DOX did not result in an increase in the apoptotic cell population compared with the single treatments. Veh = vehicle, V = VOR, D = DOX.

## DISCUSSION

Despite extensive clinical use in cancer treatment, the application of DOX is hampered by dose-dependent side effects. However, co-treatment with DOX and HDIs is considered to both enhance the efficacy and reduce the side effects because of the lower dosage. Indeed, VOR has been reported to enhance the cytotoxic effects of DOX with fewer side effects owing to a lower dosage in breast cancer cells.<sup>14</sup> In this study, we investigated a novel mechanism underlying the synergistic cytotoxic effects of VOR and DOX co-treatments in cervical cancer cells. We report that the increase in p53 acetylation in cervical cancer cells and other cancer cells induced by the co-treatment upregulates the expression level of the pro-apoptotic protein Bad, consequently leading to synergistic growth inhibition through the promotion of apoptotic death. Consistent with these data, the pro-apoptotic Bad protein was reported to promote cell death by interacting with and inhibiting the anti-apoptotic function of Bcl-2 and Bcl-XL.<sup>18</sup> These findings agree well with the case of breast cancer. For example, the treatment of breast cancer cells with DOX induces apoptosis via the downregulation of Bcl-2 and Bcl-XL,<sup>19</sup> and an upregulated expression level of Bad improves the 5-year survival rate after chemotherapy.<sup>20</sup>

We also provide the first evidence that the synergistic effects of VOR and DOX are related to the well-known p53–bad interaction. According to previous reports, p53 affects the regulation of Bcl-2 family members, including Puma,<sup>21</sup> Noxa,<sup>22</sup> Bax<sup>23</sup> and Bid,<sup>24</sup> in response to DNA damage. In particular, the human *bad* promoter has a functional p53-binding element ~6.6 kb upstream of the start codon, and the acetylation of p53 enhances its DNA-binding activity and consequent transactivation of *bad*.<sup>10–12</sup> The co-treatment of HeLa cells with VOR and DOX enhances the binding of acetylated p53 to the *bad* promoter to transactivate transcription, leading to synergistic cytotoxicity. Additionally, an accumulating body of evidence suggests that the acetylation of p53 affects the stability of p53,<sup>9,25</sup> which is likely to have some role in the synergistic cytotoxicity induced by VOR and DOX co-treatments. In contrast, the co-treatment of p53-mutated C33A cells with VOR and DOX showed no increase in the expression level of Bad or p53 acetylation, without any detectable signs of synergistic cytotoxicity.

In summary, our data provide the first evidence that the HDI VOR affects cytotoxicity by acetylating p53 instead of histone proteins. It was previously suggested that HDIs have a role in cytotoxicity through histone acetylation, relaxing the chromatin structure and making the cancer cell DNA more accessible to anticancer genotoxic drugs. In this regard, the present results provide a rationale for the potential use of new HDI anticancer drugs in future clinical trials. These findings also provide important insight into the underlying molecular mechanism of the co-treatment of VOR and DOX as an effective chemotherapy for cervical cancer. In addition, the results imply that the upregulation of Bad is a potential

therapeutic strategy for several human cancers. However, further investigations are required to determine which amino acids are acetylated after VOR and DOX co-treatments and which p53 mutation(s) are involved in this process.

## ACKNOWLEDGEMENTS

This work was supported by a National Research Foundation (NRF) grant funded by the Korea Government (MSIP) (grant no. 2012M3A9D1054666, 2013R1A2A2A01068412) and the Korea Research Institute of Bioscience and Biotechnology (KRIBB).

- 1 Tewey KM, Rowe TC, Yang L, Halligan BD, Liu LF. Adriamycin-induced DNA damage mediated by mammalian DNA topoisomerase II. *Science* 1984; **226**: 466–468.
- 2 Carvalho C, Santos RX, Cardoso S, Correia S, Oliveira PJ, Santos MS *et al*. Doxorubicin: the good, the bad and the ugly effect. *Curr Med Chem* 2009; **16**: 3267–3285.
- 3 Welander CE, Homesley HD, Barrett RJ. Combined interferon alfa and doxorubicin in the treatment of advanced cervical cancer. *Am J Obstet Gynecol* 1991; **165**: 284–290.
- 4 Marks PA. Discovery and development of SAHA as an anticancer agent. *Oncogene* 2007; **26**: 1351–1356.
- 5 Giannini G, Cabri W, Fattorusso C, Rodriquez M. Histone deacetylase inhibitors in the treatment of cancer: overview and perspectives. *Future Med Chem* 2012; **4**: 1439–1460.
- 6 Jemal A, Siegel R, Ward E, Hao Y, Xu J, Thun MJ. Cancer statistics. *CA Cancer J Clin* 2009; **59**: 225–249.
- 7 zur Hausen H. Papillomavirus infections—a major cause of human cancers. *Biochim Biophys Acta* 1996; **1288**: F55–F78.
- 8 Vousden KH, Lu X. Live or let die: the cell's response to p53. *Nat Rev Cancer* 2002; **2**: 594–604.
- 9 Feng L, Lin T, Uranishi H, Gu W, Xu Y. Functional analysis of the roles of posttranslational modifications at the p53 C terminus in regulating p53 stability and activity. *Mol Cell Biol* 2005; **25**: 5389–5395.
- 10 Gu W, Roeder RG. Activation of p53 sequence-specific DNA binding by acetylation of the p53 C-terminal domain. *Cell* 1997; **90**: 595–606.
- 11 Jiang P, Du W, Heese K, Wu M. The Bad guy cooperates with good cop p53: Bad is transcriptionally up-regulated by p53 and forms a Bad/p53 complex at the mitochondria to induce apoptosis. *Mol Cell Biol* 2006; **26**: 9071–9082.
- 12 Jiang P, Du W, Wu M. p53 and Bad: remote strangers become close friends. *Cell Res* 2007; **17**: 283–285.
- 13 Kim MS, Blake M, Baek JH, Kohlhagen G, Pommier Y, Carrier F. Inhibition of histone deacetylase increases cytotoxicity to anticancer drugs targeting DNA. *Cancer Res* 2003; **63**: 7291–7300.
- 14 Marchion DC, Bicaku E, Daud AI, Richon V, Sullivan DM, Munster PN. Sequence-specific potentiation of topoisomerase II inhibitors by the histone deacetylase inhibitor suberoylanilide hydroxamic acid. *J Cell Biochem* 2004; **92**: 223–237.
- 15 Zhao L, Au JL, Wientjes MG. Comparison of methods for evaluating drug-drug interaction. *Front Biosci (Elite Ed)* 2010; **2**: 241–249.
- 16 Lorenzo E, Ruiz-Ruiz C, Quesada AJ, Hernandez G, Rodriguez A, Lopez-Rivas A *et al*. Doxorubicin induces apoptosis and CD95 gene expression in human primary endothelial cells through a p53-dependent mechanism. *J Biol Chem* 2002; **277**: 10883–10892.
- 17 Koivusalo R, Hietanen S. The cytotoxicity of chemotherapy drugs varies in cervical cancer cells depending on the p53 status. *Cancer Biol Ther* 2004; **3**: 1177–1183.
- 18 Yang E, Zha J, Jockel J, Boise LH, Thompson CB, Korsmeyer SJ. Bad, a heterodimeric partner for Bcl-XL and Bcl-2, displaces Bax and promotes cell death. *Cell* 1995; **80**: 285–291.
- 19 Simoes-Wust AP, Schurpf T, Hall J, Stahel RA, Zangemeister-Wittke U. Bcl-2/bcl-xL bispecific antisense treatment sensitizes breast carcinoma cells to doxorubicin, paclitaxel and cyclophosphamide. *Breast Cancer Res Treat* 2002; **76**: 157–166.
- 20 Cannings E, Kirkegaard T, Tovey SM, Dunne B, Cooke TG, Bartlett JM. Bad expression predicts outcome in patients treated with tamoxifen. *Breast Cancer Res Treat* 2007; **102**: 173–179.

- 21 Nakano K, Vousden KH. PUMA, a novel proapoptotic gene, is induced by p53. *Mol Cell* 2001; **7**: 683–694.
- 22 Oda E, Ohki R, Murasawa H, Nemoto J, Shibue T, Yamashita T *et al*. Noxa, a BH3-only member of the Bcl-2 family and candidate mediator of p53-induced apoptosis. *Science* 2000; **288**: 1053–1058.
- 23 Miyashita T, Reed JC. Tumor suppressor p53 is a direct transcriptional activator of the human bax gene. *Cell* 1995; **80**: 293–299.
- 24 Sax JK, Fei P, Murphy ME, Bernhard E, Korsmeyer SJ, El-Deiry WS. BID regulation by p53 contributes to chemosensitivity. *Nat Cell Biol* 2002; **4**: 842–849.
- 25 Ito A, Kawaguchi Y, Lai CH, Kovacs JJ, Higashimoto Y, Appella E *et al*. MDM2-HDAC1-mediated deacetylation of p53 is required for its degradation. *EMBO J* 2002; **21**: 6236–6245.



**This work is licensed under a Creative Commons Attribution-NonCommercial-NoDerivs 3.0 Unported License. To view a copy of this license, visit <http://creativecommons.org/licenses/by-nc-nd/3.0/>**

Supplementary Information accompanies the paper on Experimental & Molecular Medicine website (<http://www.nature.com/emm>)